

Faraday Discussions

Accepted Manuscript



This manuscript will be presented and discussed at a forthcoming Faraday Discussion meeting. All delegates can contribute to the discussion which will be included in the final volume.

Register now to attend! Full details of all upcoming meetings: <http://rsc.li/fd-upcoming-meetings>



This is an *Accepted Manuscript*, which has been through the Royal Society of Chemistry peer review process and has been accepted for publication.

Accepted Manuscripts are published online shortly after acceptance, before technical editing, formatting and proof reading. Using this free service, authors can make their results available to the community, in citable form, before we publish the edited article. We will replace this *Accepted Manuscript* with the edited and formatted *Advance Article* as soon as it is available.

You can find more information about *Accepted Manuscripts* in the [Information for Authors](#).

Please note that technical editing may introduce minor changes to the text and/or graphics, which may alter content. The journal's standard [Terms & Conditions](#) and the [Ethical guidelines](#) still apply. In no event shall the Royal Society of Chemistry be held responsible for any errors or omissions in this *Accepted Manuscript* or any consequences arising from the use of any information it contains.

Spontaneous formation of metallic nanostructures on Highly Oriented Pyrolytic Graphite (HOPG): an ab-initio and experimental study

Maria F. Juarez^{*1}, Silvina Fuentes^{2,3}, Germán J. Soldano¹, Lucia Avalor^{2,3}, and Elizabeth Santos^{1,3}

¹*Institute of Theoretical Chemistry, Ulm University, D-89069 Ulm, Germany.*

²*Facultad de Ciencias Exactas y Naturales, Universidad Nacional de Catamarca*

³*Instituto de Física Enrique Gaviola (IFEG-CONICET), Facultad de Matemática, Astronomía y Física, FaMAF-UNC, 5000 Córdoba, Argentina.*

Abstract

We have investigated the decoration of step-edges of HOPG by Ag, Au and Pt using experimental and theoretical approaches. Metallic nanowires can be formed on bare or functionalized step-edges. Energy dispersion analysis indicates the presence of oxygenated groups. The experiments showed that nanowires can be obtained with the three metals along the step-edges, but the shapes and morphologies are very different. We have found that the interaction between the metal wires and the carbon follows the sequence: Pt>Au>Ag. The electronic redistribution between the atoms participating in the bond between the metallic nanowire and the step-edges shows a complicated pattern. The density of electronic states projected on the different atoms indicates that there are different orbitals participating in the bonds.

Introduction

Nanostructures are promising materials because of the capability to tune their properties by changing their morphology. One of the most interesting methods for their synthesis is the deposition on highly oriented pyrolytic graphite (HOPG). The topology of nanostructures resulting from metal deposition strongly depends on the interactions between metal-substrate, metal-metal and on the chemical environment. In the case of metallic substrates, pseudomorphic layer – by – layer deposits are usually obtained because of the strong metal-substrate interactions. On the contrary, metals interact very weakly with the coordinately saturated graphite basal plane surfaces; therefore the deposits are rarely epitaxially oriented on HOPG. In this case, the deposition process occurs mostly by a Volmer-Weber mechanism [1], i.e., an instantaneous nucleation and subsequent three-dimensional growth mode of deposition. A variety of shapes and sizes can be obtained depending on the pre-treatment and environment used for the deposition.

The group of Penner has performed a systematic investigation to find appropriate conditions in order to obtain either narrowly dispersed in size homogeneously distributed metal nanoparticles on atomically smooth HOPG [2-5], and also dimensionally uniform nanowires (NW) on step-defects of HOPG [6-10]. Other groups were also very active in this field [11-21]. Metallic nanostructures on HOPG have been prepared by various methods such as chemical vapor deposition (CVD) using organometallic precursors [19], physical vapor deposition (PVD) under controlled temperature of the substrate [10], spontaneous deposition at open circuit

potential (SP-ocp) immersing the HOPG in a solution containing ions of the metal to be deposited [3,15,16,20], electrochemical deposition applying potential pulses (ED) [2-6, 11,13,14,21], electrochemical step-edge decoration (ESED) [7,8] in order to obtain NW structures, Galvanic Displacement (GD) powered by the concurrent oxidation of insoluble derivatives [9].

The group of Arvía [12, 21] have obtained palladium mesoislands on HOPG with different shapes depending on the selected potential window for the electrodeposition. This growth mode change was attributed to the influence of chloride adsorbed on gold islands. These both nanostructures show markedly different catalytic activity for the oxygen reduction reaction. There is evidence from energy dispersive X-ray analysis (EDX) that chloride is also present in spontaneously deposited platinum nanoparticles [15]. Shen et al. explained this phenomenon of the presence of chloride groups and internal charges in the nanoparticle by an incomplete reduction in the spontaneous deposition. They proposed that the existent of incompletely oxidized functionalities at the step edges, other defects of the delaminated graphite layer and the hydrogen atoms formed on HOPG surface could be part of the driving force for the electroless Pt deposition.

ED produces highly monodispersed nanoparticles (NP) homogeneously distributed on the whole surface, while SP-ocp preferentially conduces to deposit on defects forming NW structures. Cross et al. [10] used ensembles of 2-15 nm diameter gold nanoparticles obtained by PVD as nucleation templates for the preparation by ESED of gold nanowires.

Pre-oxidizing HOPG by anodic current at high potentials can eliminate spontaneous deposition [3, 15, 16]. In some cases, a chemical [22], physical or electrochemical [7] pre-treatment of the HOPG is performed to induce defects, which are more active for the deposition. We can distinguish between two different domains on the surface: terraces where the carbon atoms are sp^2 bonded, and step-edges that have chemically active dangling bonds [18]. On one hand, by applying a positive potential the defects can react to form carbonyls, ethers, hydroxyls, and other oxygen containing functionalities [7,19]. On the other hand, if the applied potential is enough high, a completed oxidation of the defects takes place and the spontaneous reduction of the metal cannot occur. A major task in the state of art of this topic is to control the structure and functionalization of step-edges.

In previous works, we have performed ab-initio investigations of both freestanding metal NW [23] and supported on step-edges [24, 25]. More recently, we have found that in O_2/H_2 atmosphere, the graphene edges are mainly oxidized [26]. On the armchair edges, the terminal carbons are carboxyl groups, but on the zigzag edges, we have found stable ketones and aldehyde groups.

Now in this work, we focus on NW structures preferentially formed on functionalized step-edges by spontaneous deposition. Our goal is to understand the driving forces, which produces such structures and disentangle the metal/metal and metal/substrate interactions on perfectly hydrogenated and oxidized edges. We shall compare the stability of nanowires and small clusters on the HOPG edges.

Experimental

Highly oriented pyrolytic graphite (HOPG) provided by SPI Supplies (SPI-3, 7x7x1 mm) was used as substrate for spontaneous deposition of different metals (Au, Pt and Ag). Previous to the experiments, the surfaces were prepared by cleaving the HOPG substrates and peeling off the top layers using an adhesive tape (macroporous

Hipoalergic Clear Ind. Arg). The freshly cleaved surface obtained by means of this procedure [27] shows defects consisting of atomic steps, 0.2-0.3 nm and steps of several or dozens of atomic layers [28].

The spontaneous metal deposition was carried out at open circuit potential (ocp) using different deposition times (1s, 10s, 90s, 180s). Immersion solutions of 10 mM H_2PtCl_6 (E. Merck, Schurhardt) in 0.1 M HCl, pH 2.6 were used to obtain nanostructures of Pt. In the case of Au and Ag nanostructures, solutions of 10 mM HAuCl_4 (Sigma Aldrich) and 10 mM Ag_2SO_4 (Tetrahedron) in 0.1 M H_2SO_4 (Baker analyzed-ACS. Reagent) were employed, respectively.

After the formation of the nanostructures the electrode was removed from the deposition solution and was characterized by scanning electron microscopy (SEM) and energy dispersive microanalysis (EDS) using a FEG SEM / CARL ZEISS-Sigma instrument.

The electrocatalytic activity for the hydrogen evolution reaction was qualitatively evaluated by cyclic voltammetry at a scan rate of 0.010 V/s and 0.050V/s in a 0.5 M solution of H_2SO_4 (prepared from 98.2 % purity Baker Analyzed -ACS. Reagent). The electrochemical experiments were performed with a potentiostat - Metrohm - Autolab Galvanostat, Model PGSTAT302/302N at 25 ± 1 ° C.

Computational Details

Periodic density functional theory (DFT) calculations based on plane waves have been performed as implemented in the DACAPO code [29]. The electron-ion interactions were accounted through ultrasoft pseudopotentials [30], while the valence electrons were treated within the generalized gradient approximation (GGA) in the version of Perdew, Burke and Ernzerhof (PBE) [31]. An energy cutoff of 450 eV was used with a (12x1x1) k-points Monkhorst-Pack grid [32] for zigzag and armchair unit cell. For the relaxations the convergence criterion was achieved when the total forces were less than 10 meV/Å.

Atomic charges were obtained using the Bader analysis method, which is an intuitive method to calculate the charge enclosed around an atom [33–34]. The software used was written by Arnaldsson et al and was obtained from ref. [35-37].

All the optimized structures and electronic density differences were plotted with XCrySDen software [38].

Modeling

We modeled the graphite steps by using graphene nanoribbons (GNRs), i.e. graphene sheets which are periodic in one direction (x axis) and truncated by two edges (in the y axis). The edges correspond to the so-called armchair and zigzag configurations. One side of the nanoribbon is closed with hydrogen and the other one is used to study the adsorption of the metal wires. The vacuum between the periodic edges, and between graphene planes is greater than 12 Å. The width of the nanoribbon (from edge to edge) was optimized previously (ref. [26]), and a distance of 9.27 Å for zigzag edges and of 8.03 Å for armchair edges was used. The carbon-carbon distance was taken from the optimized graphene lattice constant: 2.46 Å which is in excellent agreement with experimental values [39]. The two bottom layers of GNRs and the hydrogen adsorbed atoms were kept fixed and the rest was fully relaxed, i.e. the metal atoms, the graphite step and the corresponding functionalization of the ending.

Results and Discussion

1. Morphological Characterization

Figure 1 shows SEM images obtained after spontaneous deposition of Au at different times. The decoration of step-edges with NPs of homogeneous size is evident from these pictures. The NPs coalesce into continuous NWs at large deposition times. NWs of about 2 μm length and 250 nm width were obtained after 3 minutes.

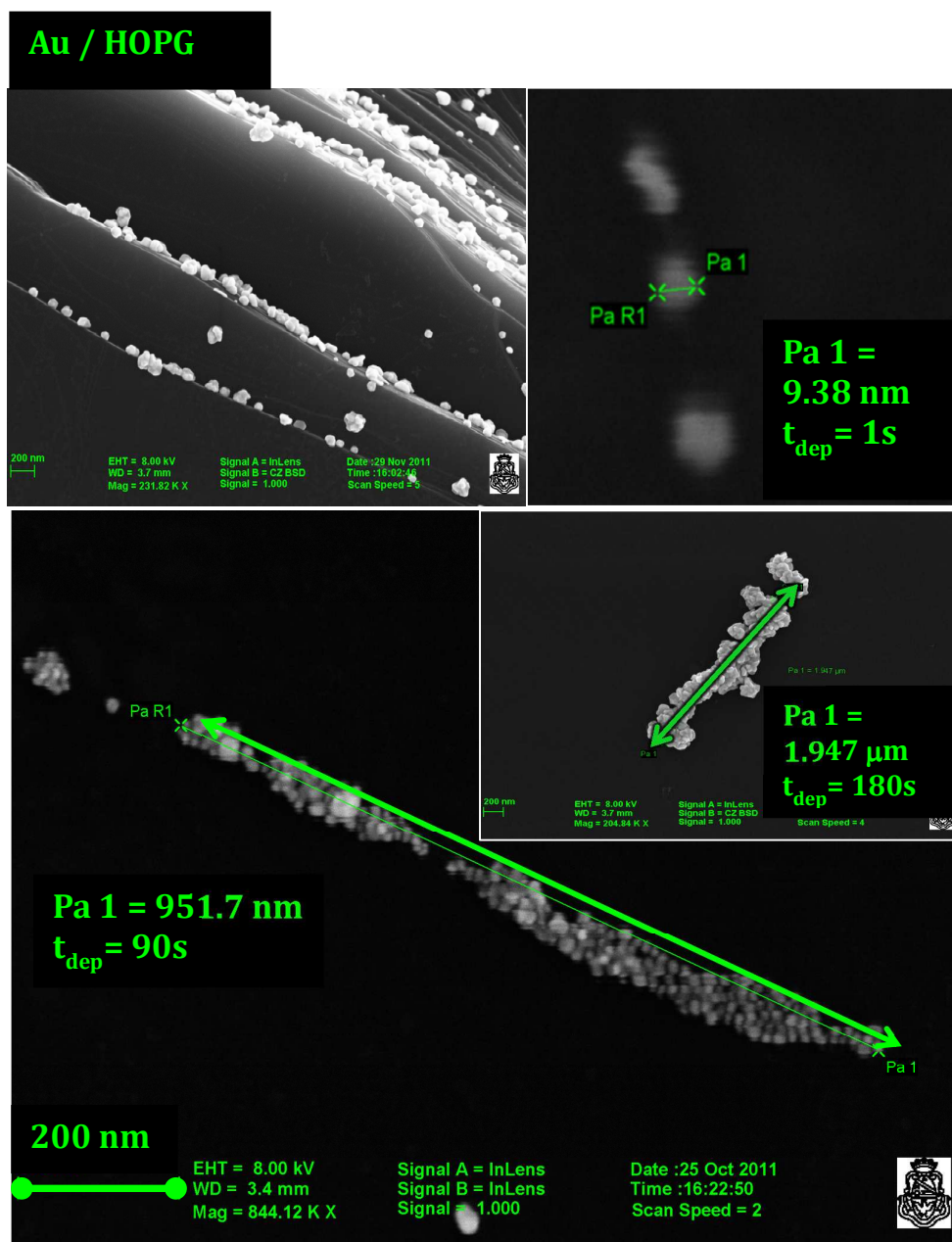


Figure 1. SEM images of Au deposited on HOPG at different times.

After peeling the HOPG, besides carbon the energy dispersive microanalysis of the fresh surface also shows traces of oxygen (Figure 2, upper part). After immersing the

HOPG in the deposition solution containing HAuCl_4 , the ED spectrum evidences the presence of Au and an increase of oxygen (Figure 2 bottom). It is possible that during the metal growth, the functionalization of the defects simultaneously takes place. Therefore, carbonyls, ethers or hydroxyl groups can be formed, supplying the necessary reducing equivalents to deposit the metal.

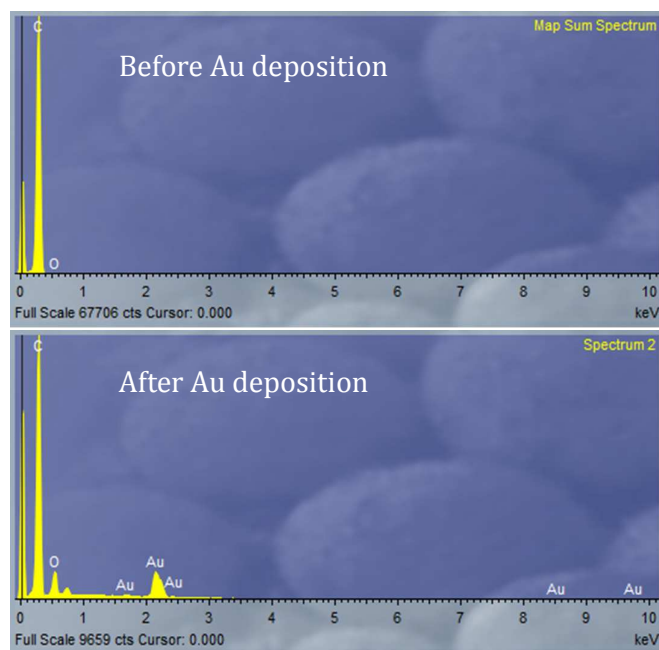


Figure 2. Energy dispersive spectra (EDS) obtained immediately after delamination of the HOPG plane (upper part), and after electroless Au deposition by immersion of the HOPG in a solution containing HAuCl_4 (bottom part).

Figure 3 shows SEM images of SD-ocp of Pt at different times. Similar to Au, Pt mainly nucleates on the step-edges defects of the HOPG. However, at longer deposition times, the NPs coalesce stronger than in the case of Au. They form almost spherical conglomerates and the NWs are shorter than for Au. There is also the tendency to form circular structures, as observed previously by Zoval et al. [3]. The EDS shows the presence of Pt and small amounts of chloride. A similar situation has been observed by Gimeno et al. [21] for Pd deposition on HOPG. They explained that clusters initially formed acquire a compact round disk shape, because the adsorbed chloride assists the isotropic interterrace surface diffusion of palladium adatoms. In the present case, the enhancement of Pt adatom surface diffusion promoted by chloride ions can also explain the appearance of compact rounded islands. Shen et al. [15] propose that the reduction of PtCl_6^{2-} to Pt is incomplete in the spontaneous deposition process. Therefore, there is still the possibility that chloride remain attached to Pt NPs.

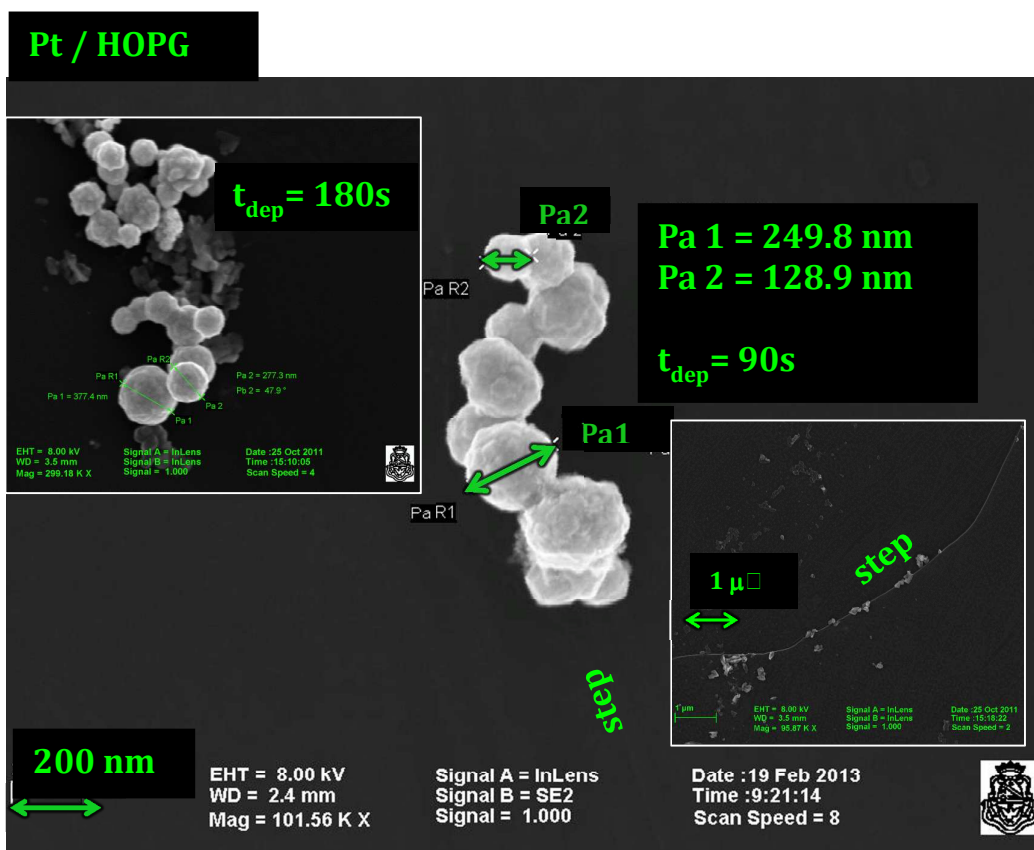


Figure 3. SEM images of Pt deposited on HOPG at different times.

In the case of Ag deposited spontaneously on HOPG, the nucleation also starts on the step-edges, but the growth can also occur in directions perpendicular to defects, as can be observed in Figure 4. Although NWs are also formed at longer deposition times, their structure is irregular and porous-like. They seem to be formed by cubic nanocrystals linked by the vertices, such as can be observed from the zoom of the image shown in the inset of Fig. 4. The cubic shape indicates that the nanocrystals expose predominantly (100) facets. EDS analysis shows besides Ag, the presence of traces of Sulphur, probably coming from the sulphate electrolyte used for the deposition and an incomplete reduction. Although Ag display a unique oxidation states, it can occur a similar phenomenon as in the case of Pt. Traces of Ag_2SO_4 salt could be also contained in the metallic NPs.

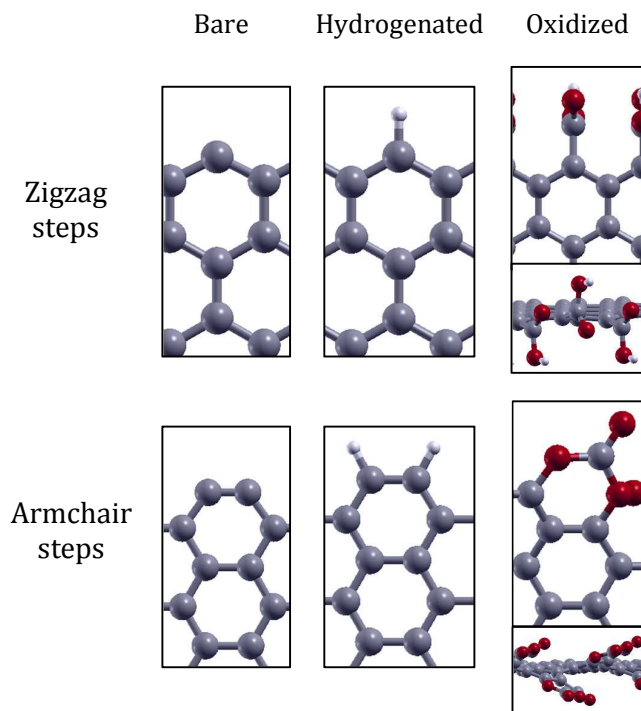
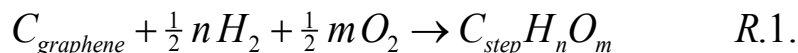


Figure 5. Top views of the optimized structures of the zigzag (upper part) and armchair (bottom) steps: bare (left), hydrogenated (middle), and oxidized (right) terminations. A side view has been included for the oxidized steps in order to show the three-dimensional arrangement of the functional groups.

The stability of the structures has been evaluated by calculating the energy for the formation reaction:



$$\Delta E_{\text{form}} = \frac{E(C_{\text{step}} H_n O_m) - E(C_{\text{graphene}}) + \frac{1}{2} n E(H_2) + \frac{1}{2} m E(O_2)}{L_x} \quad (1)$$

where $C_{\text{step}} H_n O_m$ is the functionalized graphene step, C_{graphene} is an infinite layer of graphene, and H_2 and O_2 are the hydrogen and oxygen molecules in the vacuum, respectively. According to this definition, a positive formation energy means that energy is required in order to create a functionalized step. For a sake of comparison, all the energy values have been normalized by the length L_x of the corresponding step, making possible to compare the results obtained in zigzag and armchair steps. The formation energies of systems shown in Fig. 5 are collected in Table 1.

The steps with unpaired electrons (the bare steps) are the most unstable, whereas the oxidized steps are the most stable ones. The armchair steps are slightly more stable than zigzag steps in all the studied cases. However, the differences enlarge if we consider the length per step atom. The separation between carbon atoms in zigzag steps is larger than in armchair systems (2.46 Å vs 2.13 Å), making the formation energy per atom bigger in the zigzag steps.

Table 1. Formation energies of the functionalized graphene steps shown in Figure 5.

Step		ΔE_{form} (eV/Å)
Zigzag	Bare	1.08
	Hydrogenated	0.088
	Oxidized	-0.95
Armchair	Bare	0.98
	Hydrogenated	0.038
	Oxidized	-1.14

The formation energies of the hydrogenated endings are very close to zero, denoting that energy required to cleavage the graphene layer is compensate with newly formed C-H bonds.

3. Metal nanowires on graphene steps: Energetics, and structural analysis

In this part, we shall consider separately different aspect of the adsorption of gold, silver, and platinum metal to form wires on the steps. We shall start with the geometric analysis of the optimized structures and we shall continue with energetics of the adsorption process.

On the bare steps, the geometrical arrangement of the atoms was the same for the three considered metals. A schematic plot of the geometries is shown in Figure 6. Table 2 presents the most important bond lengths and angles of the metal wires adsorbed on different graphene steps.

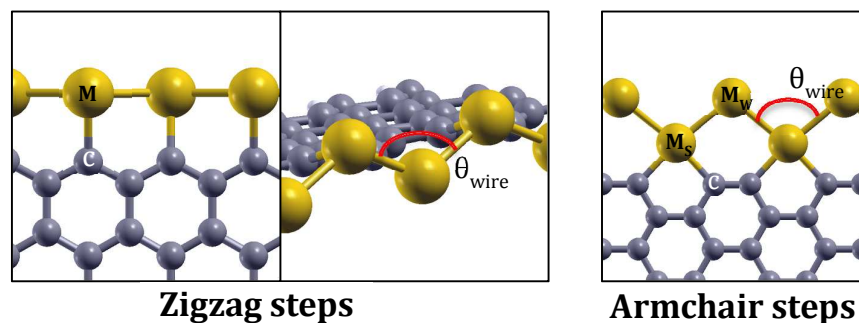


Figure 6. Top view of the optimized metal wires adsorbed on bare zigzag (left) and armchair (right) steps. A side view of the metal wire in the zigzag step has been included in order to show the lateral structure of the wire.

On the zigzag steps, every metal atom is bound to a carbon atom with a distance between them that is shorter than metal-metal bond distances in gold, platinum and silver free-standing wires. Therefore, and in order to improve the bond between the metal atoms, the wire loses its lineal geometry. As we can observe in Table 2, the larger distortion angles θ_{wire} correspond to the metal wires supported on armchair steps, where the metal/metal bond length is even larger than in zigzag steps. The carbon/metal atom distance decreases in the sequence: Ag>Au>Pt, in zigzag and armchair steps.

Table 2. Geometrical parameters of the metal nanowires supported on bare, hydrogenated and oxidized graphene steps. The corresponding values for free standing wires are shown for sake of comparison.

1) Ag							
	Free	Bare		Hydrogenated			
		Zigzag	Armchair	Zigzag	Armchair		
$d_{MM}/\text{\AA}$	2.70	2.75	2.79	2.88	2.72		
θ_{wire}	180	127	99	117	103		
$d_{CM}/\text{\AA}$	--	2.16	2.17	2.16	2.17		
2) Au							
	Free	Bare		Hydrogenated			
		Zigzag	Armchair	Zigzag	Armchair		
$d_{MM}/\text{\AA}$	2.66	2.74	2.74	2.60	2.84		
θ_{wire}	180	128	102	142	97		
$d_{CM}/\text{\AA}$	--	2.09	2.12	2.13	2.13		
3) Pt							
	Free	Bare		Hydrogenated		Oxidized	
		Zigzag	Armchair	Zigzag	Armchair	Zigzag	Armchair
$d_{MM}/\text{\AA}$	2.41	2.55	2.60	2.55	2.66	2.76	2.49 ^a
θ_{wire}	180	150	110	148	106	126	151 ^b
$d_{CM}/\text{\AA}$	--	1.94	2.07	1.97	2.09	2.01	2.08

^a The value corresponds to the average of values obtained for the four distinguishable Pt atoms.

^b The value corresponds to the angle between the atoms in the ends and the middle of the wire.

The adsorption of metal wires was also studied in the hydrogenated steps. The optimized systems are plotted in Figure 7. It is straightforward to notice that the final geometry depends on the nature of metal atoms.

On the hydrogenated armchair steps, the final structure is similar for the three metals. In these systems, one of the hydrogen atoms is bound to the two metal atoms. This interaction is stronger in platinum than in silver, and it increases the metal/metal bond length in the former case, and makes the opposite in the later case. We have also found a correlation between the increase in the metal/metal bond length and the reduction of angle θ_{wire} .

Another investigated system is the platinum nanowire supported on oxidized steps. Different views are plotted in Figure 8, in order to show the special geometries of adsorption. It is important to point out that on the zigzag steps, the platinum atoms break the carboxylic groups, take away the OH and produce new bonds with the oxygen atoms. On the armchair steps, only one metal atom (of a total of four) is bound to one lactone cycle. In this case, there are two bonds that attached the wire, one with oxygen atom outside of the ring, and the other one with most oxidized carbon atom in the lactone.

Platinum wires adsorbed on oxidized steps exhibit two different behaviours. On the zigzag steps, the nanowire is strongly attached to the step, increasing the metal/metal bond largely. On the other hand, the platinum wire supported on the armchair step is weakly adsorbed, and the final geometry of the nanowire is quite similar to the one in vacuum.

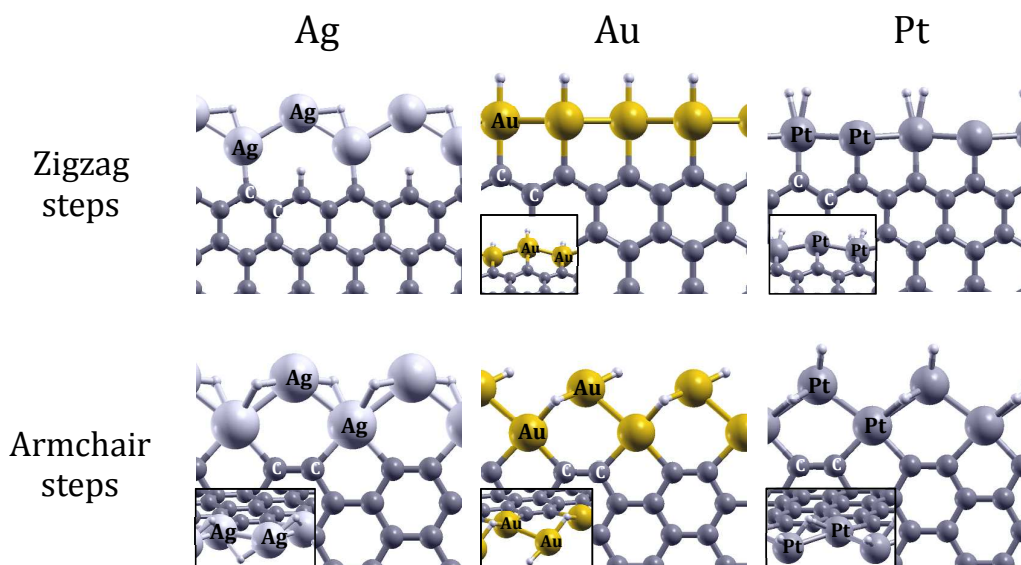


Figure 7. Top view of the optimized metal wires adsorbed on hydrogenated zigzag (upper part) and armchair (bottom) steps. Tilted and side views of the metal wire in the zigzag and armchair step have been included in order to show the lateral distortion of the nanowire structure.

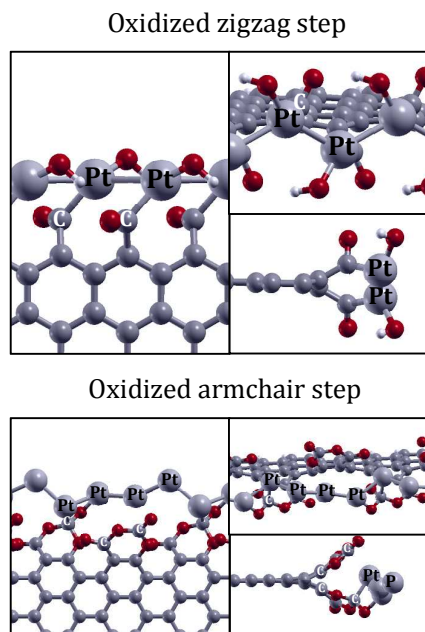


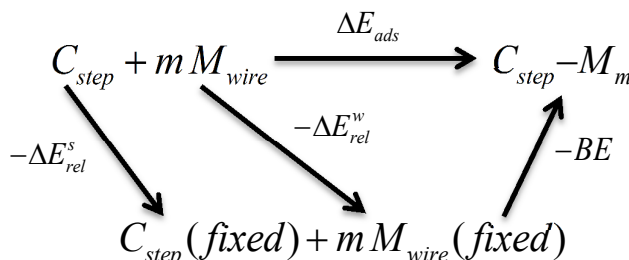
Figure 8. Top and side views of the optimized Pt metal wires adsorbed on oxidized zigzag (upper part) and armchair (bottom) steps.

In order to analyse the stability of the previous systems, we have calculated several formation reactions considering the functionalization of the steps.

-Adsorption on bare steps: The adsorption of a nanowire in a bare step can be described using the main reaction in Scheme 1. The energy of such adsorption is given by the equation

$$\Delta E_{ads} = \frac{E(C_{step}M_m) - E(C_{step}) + mE(M_{wire})}{L_x} \quad (2)$$

where $E(C_{step}M_m)$, $E(C_{step})$, and $E(M_{wire})$ are the energies of adsorbed nanowire, bare step, and free standing wire, respectively. In order to decompose the adsorption energy ΔE_{ads} in its fundamental parts, we have used a thermodynamic cycle adding three reactions: 1) the distortion of a relaxed nanowire, 2) the distortion of a relaxed step, and 3) the binding between the two unrelaxed parts (wire + step).



Scheme 1. Adsorption reaction of a nanowire in a bare step. The thermodynamic cycle decomposes the adsorption process in three different reactions: 1) distortion of the nanowire, 2) distortion of the substrate (graphene step), and 3) union of the two parts (step + wire).

The energy required to produce the distortion of the nanowires or the steps is the opposite of the relaxation energy of them, and can be described using the equations:

$$\Delta E_{rel}^s = \frac{E(C_{step}) - E(C_{step}^{fixed})}{L_x} \quad (3)$$

$$\Delta E_{rel}^w = \frac{E(M_{wire}) - E(M_{wire}^{fixed})}{L_x} \quad (4)$$

where $E(M_{wire}^{fixed})$ and $E(C_{step}^{fixed})$ are the energies of the graphene step and the metal nanowire with the same geometry as in the adsorbed system (wire+step). According to these definitions, a negative value means that the energy of the relaxed (free) substrate (or adsorbate) is lower than energy of the fixed system. Therefore, in this case, it is necessary to give energy to the system in order to modify the structure of the substrate or the adsorbate.

The final contribution to the adsorption is the binding energy between the adsorbate (nanowire) and the substrate (graphene step):

$$BE = \frac{E(C_{step}^{fixed}) + mE(M_{wire}^{fixed}) - E(C_{step}M_m)}{L_x} \quad (5)$$

It is important to notice that either the nanowire or the step, must have exactly the same geometry as in the final system, so the binding energy is only the result of the chemical interaction between the two of them. As it follows from the eq. (5), a positive value corresponds to an attractive interaction between substrate and adsorbate. From the thermodynamic cycle, the adsorption can be reconstructed as is shown in the equation:

$$\Delta E_{ads} = -BE - \Delta E_{rel}^s - \Delta E_{rel}^w$$

The energies are summarized in Table 3.

Table 3. Adsorption energies for nanowires supported on bare zigzag and armchair steps. The relaxation and binding energies as been included to decompose the adsorption energy, according to the thermodynamic cycle shown in Scheme 1.

Step	M	ΔE_{ads} (eV/Å)	BE (eV/Å)	ΔE_{rel}^w (eV/Å)	ΔE_{rel}^s (eV/Å)
Zigzag	Ag	-0.42	0.44	0.023	-0.042
	Au	-0.50	0.58	0.056	-0.133
	Pt	-1.17	1.24	-0.002	-0.064
Armchair	Ag	-0.37	0.47	0.029	-0.130
	Au	-0.63	0.76	0.042	-0.170
	Pt	-0.80	1.04	0.012	-0.254

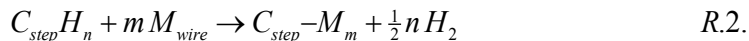
The values obtained in table 3 lead to several conclusions.

The first conclusions are about the distorsion in the geometries of the wires and steps. We have found that the relaxation energies for the nanowires are small in all the cases and they are within the DFT error (0.1 eV). The relaxation energies for the steps are larger in the armchair than in the zigzag case, being the platinum wire the one that produces the biggest distorsion.

On second place and according to the analysis of the binding energy, we have found that the interaction between the metal wires follows the sequence: Pt>Au>Ag. We want to point out here that there is a correlation between the increase in the binding energies and the reduction in the bond length d_{CM} , that follows the enhancement in the bond between the substrate and the metal nanowire.

Finally we have observed that, due to the fact the relaxation energies are mainly negligible, the adsorption energies can be estimated from the binding energies. The only exception is the platinum wire on armchair steps, where the distorsion energy is significant.

So far we have only considered the adsorption of nanowires from bare graphene steps. However, it is also possible to produce the same structures using hydrogenated or oxidized steps as starting surfaces, and removing the functional groups:

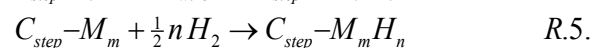
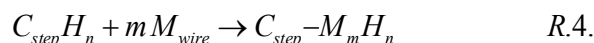


The energies of the reactions R.2 and R.3 are named ΔE_{ads2} , and ΔE_{ads3} , respectively. The values obtained for the three metal wires are provided in Table 4. According to these results, the adsorption of the nanowires needs external energy in order to completely remove the oxide from the step. A similar situation occurs with the hydrogenated steps, being the only exception the platinum wires on the zigzag steps.

Table 4. Adsorption energies for nanowires supported on bare steps as they are defined by reactions R.2 and R.3. All the energies have been normalized by the length L_x of the unit cell.

Step	M	$\Delta E_{\text{ads}2}$ (eV/Å)	$\Delta E_{\text{ads}3}$ (eV/Å)
Zigzag	Ag	0.58	1.60
	Au	0.50	1.53
	Pt	-0.17	0.85
Armchair	Ag	0.57	1.76
	Au	0.31	1.50
	Pt	0.14	1.33

-Adsorption on hydrogenated steps: Several reactions can be defined for the formation of the same system, but we shall consider only the following ones:



While both reactions have the same final product, the reactants are different and their meanings too. Reaction R.4 is the adsorption of a metal wire with partial or total displacement of hydrogen from the step. The first case corresponds to silver on zigzag steps, and in all the cases, hydrogen atoms make new bonds with the metal atoms. Reaction R.5 does not represent the adsorption of any metal atoms but of hydrogen atoms, with a chance of partial remotion of metal atoms. Again, the last case corresponds to silver on zigzag steps. The adsorption of hydrogen atoms is an important reaction that has been widely used to study the reactivity of an extensive list of systems (surfaces, modified surfaces, nanostructures).

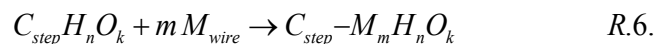
Table 5. Energies of the reactions R.4 and R.5, involving nanowires supported on hydrogenated steps. All the energies have been normalized by the length L_x of the unit cell.

Step	M	$\Delta E_{\text{hydr}1}$ (eV/Å)	$\Delta E_{\text{hydr}2}$ (eV/Å)
Zigzag	Ag	0.22	-0.36
	Au	0.45	-0.05
	Pt	-0.24	-0.08
Armchair	Ag	0.64	-0.15
	Au	0.31	-0.39
	Pt	-0.18	-0.10

The energies $\Delta E_{\text{hydr}1}$ (reaction R.4) in Table 5 indicate that the formation of these systems requires energy for gold and silver nanowires. Platinum has not only a strong interaction with the graphene steps but also with the hydrogen atoms. Therefore, the adsorption of Pt atoms compensates the breaking of the C-H bonds.

As the results for the energies $\Delta E_{\text{hydr}2}$ show in Table 5, the adsorption of hydrogen on the supported metal wires improves the stability of the systems, lowering the final energy and gaining energy after the reaction. This effect is more remarkable for silver on zigzag steps and gold on armchair endings.

-Adsorption of Pt on oxidized steps: The last reaction studied is the adsorption of a Pt wire on an oxidized step:



The energies are briefly summarized on Table 6. We have found that it is still possible to adsorb platinum on the oxidized step, but the energy obtained is smaller than in bare or hydrogenated steps. On zigzag steps, a possible explanation for this result is the large amount of energy invested on the breaking of OH group from the carboxylic ending. The situation is quite different on the armchair step, where the nanowire is attached to a lower number of atoms from the step.

Table 6. Energies of the reaction R.6, between platinum nanowires and oxidized steps. All the energies have been normalized by the length L_x of the unit cell.

Step	M	ΔE_{oxid} (eV/Å)
Zigzag	Pt	-0.14
Armchair	Pt	-0.07

4. Metal nanowires on graphene steps: Density of states (DOS), charges and electronic density differences

In this final part, we shall describe with a certain detail the nature of the bond between the metal wires and the bare zigzag and armchair steps. We shall use the results obtained through Bader analysis, electronic density difference and atomic projected DOS (pDOS). And we shall finish with a short description of the platinum wires on three functionalized graphene steps.

The atomic charges obtained through the Bader analysis are summarized in table 7. On the zigzag steps, the charge on the metal atoms depends on the nature of the metal. The largest value in this case was obtained for the silver nanowire. We have also found that the positive charges on the metal atoms correlate with the negative charge on the carbon atoms. These results suggest that there is a small charge transfer between the metal and carbon atoms.

On the armchair steps, we have two different metal atoms: M_s (closer to the step) and M_w (far from the step). On one hand, the positive charges on the atom M_s are larger than in the zigzag steps, but they are independent of the nature of the atom. But on the other hand, the charges on the atom M_w are negative and depend on the metal. As in the zigzag steps, the carbon atoms are negatively charged too.

Table 7. Bader charges for the carbon and metal atoms in the metal wires supported on bare graphene steps.

Zigzag steps				Armchair steps			
charge	Ag	Au	Pt	charge	Ag	Au	Pt
q_M	+0.19	+0.09	+0.06	q_{M_s}	+0.35	+0.36	+0.35
q_C	-0.14	-0.10	-0.07	q_{M_w}	-0.05	-0.17	-0.13
				q_C	-0.18	-0.13	-0.16

In order to get a better description, we have also used the electronic density difference defined by the equation:

$$\Delta\rho = \rho(C_{step}M_m) - \rho(C_{step}^{fixed}) + \rho(M_m^{fixed}) \quad (6)$$

where $\rho(C_{step}M_m)$, $\rho(C_{step}^{fixed})$, and $\rho(M_m^{fixed})$ are the electronic densities of the adsorbed nanowire, the fixed step and the fixed wire, both fixed at the same geometry that the adsorbed nanowire, respectively. According to this definition, a positive value corresponds to an accumulation of electrons.

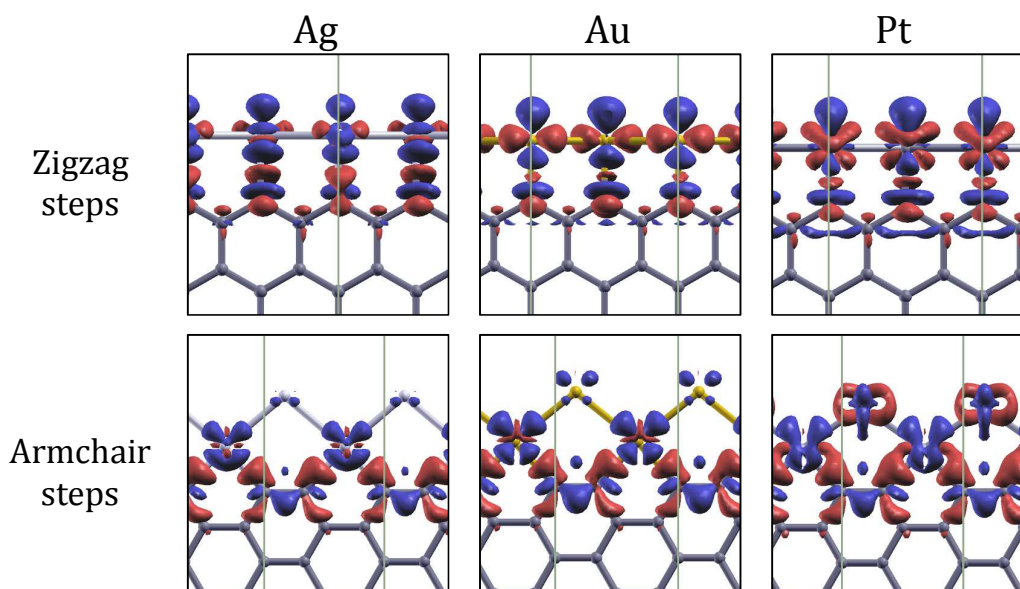


Figure 9. Top view of the electronic density difference obtained using eq. (6). Negatives (positive) values are plotted in blue (red). The isocontours correspond to a value of $0.006 \text{ electron}/\text{\AA}^3$.

Figure 9 shows the density difference obtained for the selected systems. Besides the fact that the obtained plots are complex, we can observe some trends. In all the systems studied there is an accumulation of electrons between the carbon and metal atoms. In the zigzag steps, there is also an increase of density between the metal atoms in the wire.

On the armchair we can observe that the density in the atom M_s remains constant in the three metal, but it is rather different for the atom M_w . This observation corroborates the result obtain with the Bader analysis.

It is important to notice that, even when the atomic charges calculated with Bader method are small, the local distribution of electron can be rather complex and full of redistributions between different atoms and orbitals in the same atom.

Finally, we want to point out that the complex structure of the pictures indicates that there are more than one kind of orbitals participating in the bonds, and changing their populations during the adsorption.

To complete the analysis of the nature of the wire/step bond, we have projected the DOS in the sp and d bands of the metal atoms, and the sp band of the carbon atoms. Figure 10 shows the results for the nanowires supported on the zigzag and armchair steps.

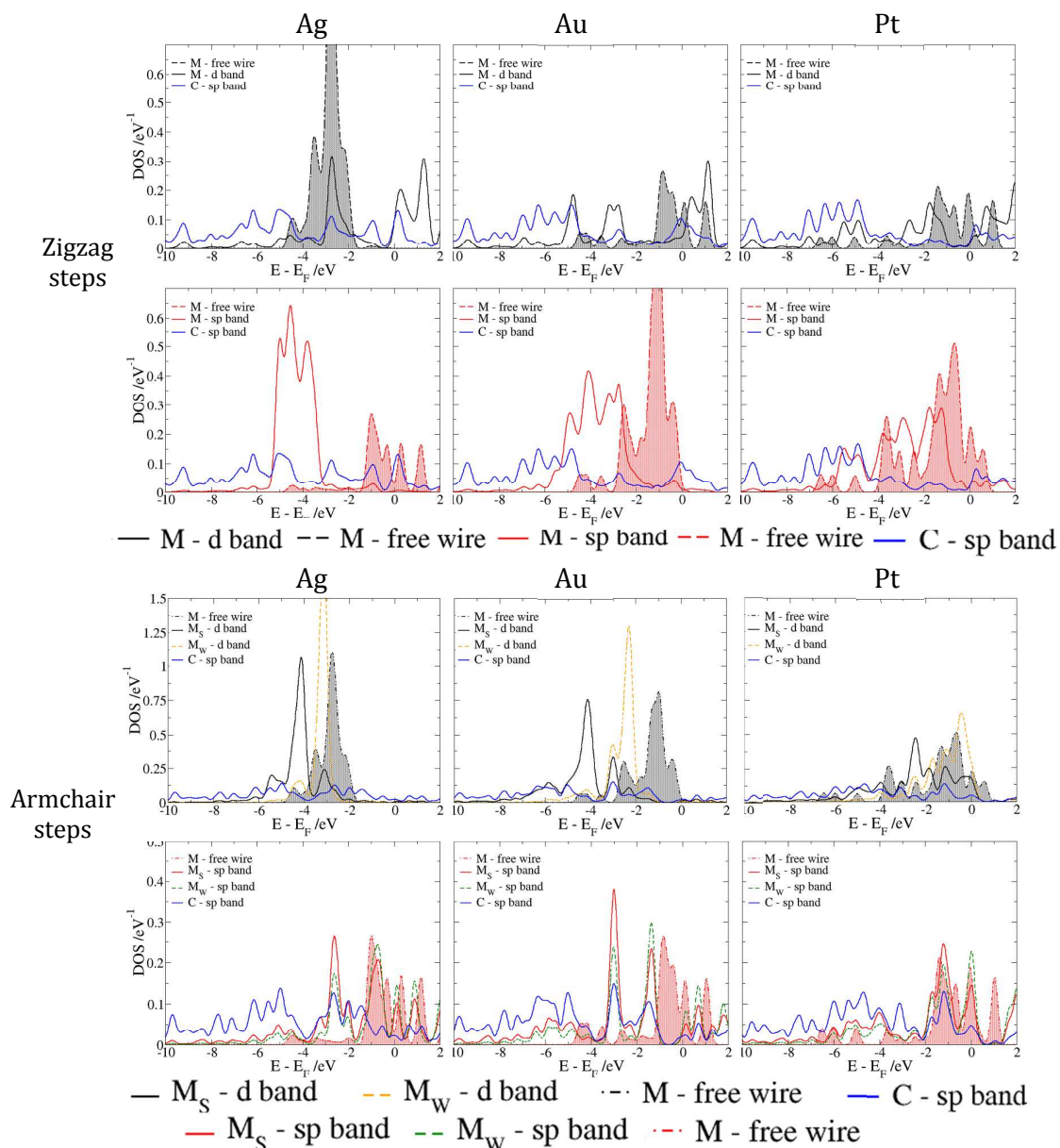


Figure 10. Atomic projected DOS of metal nanowires adsorbed on bare graphene steps. The projections are plotted in different colors as follows: blue lines for the sp band of C atom; black and red lines for the metal d and sp band, respectively. The filled curves have added for a sake of comparison, and correspond to the orbitals in the free standing wire.

On the zigzag steps, the d and sp bands of the metal atoms contribute equally to the bond with the step, whereas on the armchair steps, the sp band has a minor role.

After the adsorption of the nanowire, we can observe a shift in the d bands to lower energies, with the only exception of silver on zigzag steps. On the armchair steps, the atom M_S has larger shift than the atom M_W .

Finally it is interesting to analyse the case of the silver nanowire adsorbed on the zigzag step. Atomic charges have shown that the silver atom is positively charged, with a small charge of +0.19. However, the density difference indicates that the situation is more complicated, and there is also an accumulation of electrons in the

silver atom. The pDOS supports this observation and gives more information. We can observe in Fig. 10 that the occupation of the d band is smaller on the supported wire than on the free-standing wire. In Fig. 10, we can also notice that the loss of electrons in the d band is compensated by an increase in the DOS of the sp band. Therefore, the net charge in the silver is closer to zero but the electron difference shows that there is an important redistribution of the electrons.

Table 8. Bader charges for the carbon and Pt atoms in the platinum nanowires supported on bare, hydrogenated, and oxidized graphene steps.

	Zigzag steps			Armchair steps			
charge	Bare	Hydrogenated	Oxidized	charge	Bare	Hydrogenated	Oxidized
q_M	+0.06	+0.15	+0.54	q_{Ms}	+0.35	+0.26	+0.21 ^a
q_C	-0.07	-0.15	+1.6	q_{Mw}	-0.13	+0.05	-0.06 ^b
				q_C	-0.16	-0.21	+2.9 ^c

We shall conclude this section with the analysis of platinum wires attached to different graphene edges. The Bader charges for the platinum and carbon atoms in these systems are shown in Table 8.

The calculated charges of platinum atoms present two interesting cases. On the oxidized steps we found the most positive charge of the selected systems, whereas on the oxidized armchair step, the platinum shows a significant lowering of the positive charge. In the former case, the large charge is due to the bond between the platinum atom and a oxygen atom (from a OH group). However, in the second case the nanowire is weakly adsorbed through a bond between the platinum atom and the oxidized carbon atom.

The DOS of the platinum nanowires adsorbed on the oxidized steps is shown in Figure 11. There, the DOS have been projected in the atomic orbitals as follows: d and sp band of platinum atoms, sp band of carbon, p band of oxygen. We have only considered the carbon and oxygen atoms directly bound to the platinum atoms. In order to improve the analysis, we have also included pDOS of the carbon and oxygen atoms in the relaxed, oxidized step (without metal atoms), and of the platinum atom in the free standing wire.

The comparison between the bands of carbon and oxygen atoms with and without the metal atoms, allow us to conclude that the oxygen atom has a fundamental role in the formation of the new bonds. The new orbitals can be found at energies closer to the Fermi level. On the armchair steps, we can also see an important new state below 4 eV of the Fermi level.

The orbitals of the platinum atoms in the nanowire supported in the armchair step present small changes in comparison with the orbitals of the free standing wires. This result is in line with our previous observation that the nanowire is weakly attached to edge and the structure of the wire is slightly modified.

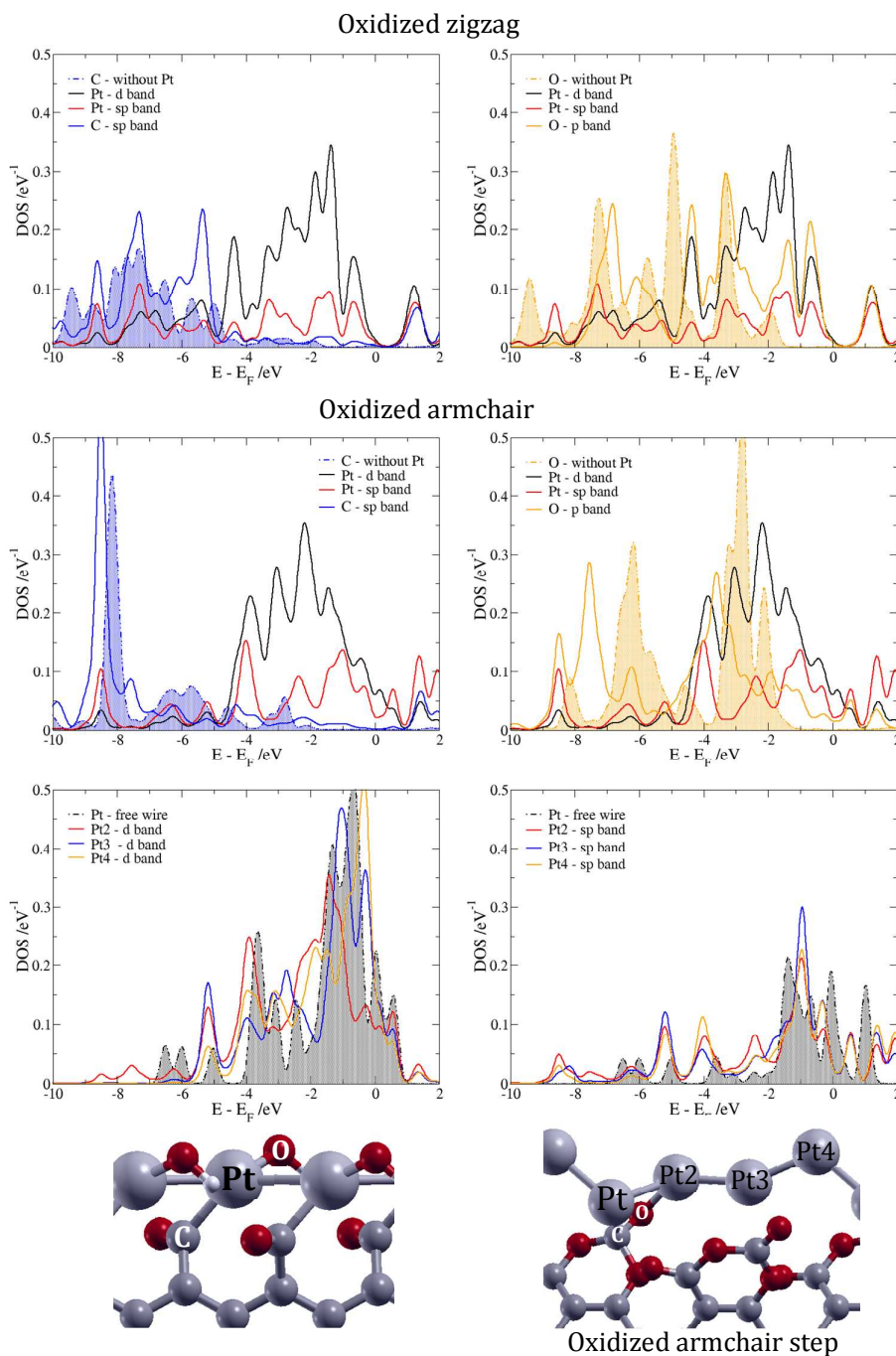


Figure 11. Atomic projected DOS of Pt nanowires adsorbed on oxidized graphene steps. The projections are plotted in different colors as follows: blue lines for the sp band of C atom; black and red lines for the metal d and sp band, respectively. The filled curves have added for a sake of comparison, and correspond to the orbitals in the free standing wire.

Conclusions

We have contrasted two totally different approaches: an experimental overview of spontaneous deposition of Ag, Au and Pt and theoretical investigations of the initial stages of the decoration of step-edges of HOPG with those metals.

The experiments showed that nanowires can be obtained with the three metals along the step-edges, but the shapes and morphologies are very different. While Au can form very long and thin nanowires by merging small nanoparticles, in the case of Pt there is a tendency of the nanoparticles to coalesce in much larger and almost spherical clusters, probably facilitated by the presence of chloride anions. The decoration with Ag is less favourable and frequently the growth of the nanowires occurs perpendicular to the step-edges with nanocrystals showing preferentially (100) facets. Energy dispersive microanalysis showed the presence of oxygen, indicating that functionalities such as carboxyls, ethers, aldehydes or hydroxyls could be present at defects.

Theoretical calculations of nanowires formation on bare and functionalized step-edges have been performed for different morphologies and chemical groups. We have found that the interaction between the metal wires and the carbon follows the sequence: Pt>Au>Ag. In the case of hydrogenated edges, the formation of nanowires requires energy for gold and silver nanowires. Platinum has not only a strong interaction with the step-edges but also with the hydrogen atoms. Therefore, the adsorption of Pt atoms compensates the breaking of the C-H bonds. We have found that it is still possible to adsorb platinum on the oxidized step, but the energy obtained is smaller than in bare or hydrogenated steps. The old idea that the driving force for electroless metal deposition derives from the supply of electrons by incompletely oxidized functionalities is partially confirmed from the charge and charge difference calculations. However, the landscape is much more complicated. It is important to notice that, even when the atomic charges calculated with Bader method are small, the local distribution of electron can be rather complex and full of redistributions between different atoms and orbitals in the same atom. Finally, we want to point out that the complex structure of the pictures indicates that there are more than one kind of orbitals participating in the bonds, and changing their populations during the adsorption, as confirmed from the density of states projected on the different atoms.

In this contribution, we have set the starting points at the two extreme of a bridge between experiments and theory to understand the metal decoration of step-edges on HOPG. On one hand, an analysis under systematic control of the experimental conditions is required. On the other hand, the inclusion of a more realistic environment such as the presence of chloride or solvent molecules is necessary in the theoretical description.

Acknowledgments

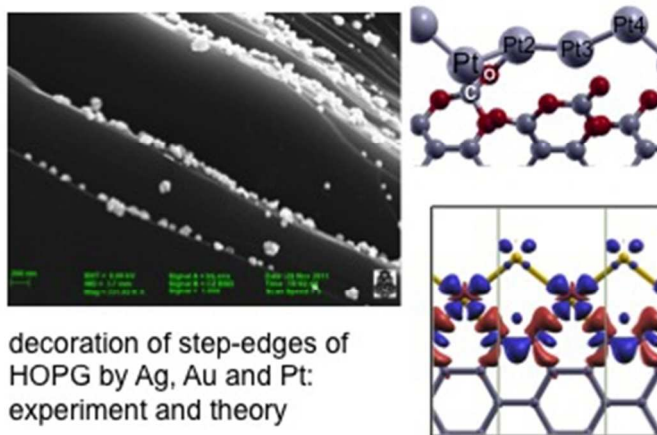
This work is part of the research network FOR1376 financed by the Deutsche Forschungsgemeinschaft. We thank PIP-CONICET 112-201001-00411, PICT-2008-00088 and PICT- 2012-2324 (Agencia Nacional de Promoción Científica y Tecnológica, FONCYT, préstamo BID) for support.

We are also grateful for support from FaMAF for the funding through the Segundo Plan de Inversiones para Equipamientos 2010–2011 and a generous grant of computing time from the Baden-Württemberg.

References

- [1] E. Budevski, G. Staikov and W.J. Lorenz, "Electrochemical Phase Formation and Growth", VCH Verlagsgesellschaft GmbH, Weinheim, 1996.
- [2] J.V. Zoval, R.M. Stiger, P.R. Biernacki and R. M. Penner, *J. Phys. Chem.*, 1996, **100**, 837.
- [3] J.V. Zoval, J. Lee, S. Gorer and R. M. Penner, *J. Phys. Chem. B*, 1998, **102**, 1166.
- [4] H. Liu and R.M. Penner, *J. Phys. Chem. B*, 2000, **104**, 9131.
- [5] H. Liu, F. Favier, K. Ng, M.P. Zach and R.M. Penner, *Electrochim. Acta*, 2001, **47**, 671.
- [6] R.M. Penner, *J. Phys. Chem. B*, 2002, **106**, 3339.
- [7] E.C. Walter, B.J. Murray, F. Favier, G. Kaltenpoth, M. Grunze, and R.M. Penner, *J. Phys. Chem. B*, 2002, **106**, 11407.
- [8] E. C. Walter, M. P. Zach, F. Favier, B. J. Murray, K. Inazu, J. C. Hemminger, and R. M. Penner, *Chem. Phys. Chem.*, 2003, **4**, 131.
- [9] R. A. W. Dryfe, E. C. Walter, and R. M. Penner, *ChemPhysChem*, 2004, **5**, 1879.
- [10] C. E. Cross, J. C. Hemminger, and R. M. Penner, *Langmuir*, 2007, **23**, 10372.
- [11] M. S. El-Deab, T. Sotomura, and T. Ohsaka, *J. Electrochem. Soc.*, 2005, **152**, C730.
- [12] A. Hernández Creus, Y. Gimeno, P. Díaz, L. Vázquez, S. González, R.C. Salvarezza, and A.J. Arvia, *J. Phys. Chem. B*, 2004, **108**, 10785.
- [13] T. Brülle, and U. Stimming, *J. Electroanal. Chem.*, 2009, **636**, 10.
- [14] T. Brülle, W. Ju, Ph. Niedermayr, A. Denisenko, O. Paschos, O. Schneider, and U. Stimming, *Molecules*, 2011, **16**, 10059.
- [15] P. Shen, N. Chi, Kwong-Yu Chan, and D.L. Phillips, *Appl. Surf. Science*, 2001, **172**, 159.
- [16] G. Lu, and G. Zangari, *Electrochim. Acta*, 2006, **51**, 2531.
- [17] O. V. Cherstiouk, P. A. Simonov and E. R. Savinova, *Electrochim. Acta*, 2003, **48**, 3851.
- [18] Han-Bo-Ram Lee, S. H. Baeck, Th. F. Jaramillo, and S. F. Bent, *Nano Lett.*, 2013, **13**, 457.
- [19] M. Aktary, Ch. E. Lee, Y. Xing, S. H. Bergens, and M. T. McDermott, *Langmuir*, 2000, **16**, 5837.
- [20] P.M. Quaino, M.R. Gennero de Chialvo, M.E. Vela, and R.C. Salvarezza, *J. Argent. Chem. Soc.*, 2005, **93**, 215.
- [21] Y. Gimeno, A. Hernández Creus, P. Carro, S. González, R. C. Salvarezza, and A. J. Arvia, *J. Phys. Chem. B*, 2002, **106**, 4232.
- [22] W. Xia, C. Jin, S. Kundu, and M. Muhler, *Carbon*, 2009, **47**, 919.
- [23] E. Santos, P. Quaino, G. Soldano, and W. Schmickler, *Electrochem. Commun.*, 2009, **11**, 1764.
- [24] G. J. Soldano, P. Quaino, E. Santos, and Wolfgang Schmickler, *J. Phys. Chem. C*, 2013, **117**, 19239.
- [25] G. J. Soldano, P. Quaino, E. Santos, and Wolfgang Schmickler, *Chem. Phys. Chem.*, 2010, **11**, 2361.
- [26] G. Soldano, F. Juarez, B. Teo, and E. Santos, "Stability and structure of oxidized graphene edges in an O₂ and H₂ environment from ab initio thermodynamics", (submitted).
- [27] H. Chang and A. J. Bard, *Langmuir*, 1991, **7**, 1143.
- [28] N. Patel, M. G. Collignon, M. A. O'Connell, W. O. Hung, K. McKelvey, J. V. Macpherson and P. R. Unwin, *J. Am. Chem. Soc.*, 2012, **134**, 20117.
- [29] <http://www.fysik.dtu.dk/campos> (accessed Oct 2007).
- [30] D. Vanderbilt, *Phys. Rev. B*, 1990, **41**, 7892.
- [31] J.P. Perdew, K. Burke, M. Ernzerhof, *Phys. Rev. Lett.*, 1996, **77**, 3865.
- [32] J.H. Monkhorst, D.J. Pack, *Phys. Rev. B*, 1976, **13**, 5188.
- [33] R.F.W. Bader, W.H. Henneker, P.E. Cade, *J. Chem. Phys.*, 1967, **46**, 3341.
- [34] R.F.W. Bader, P.E. Cade, P.M. Beddall, *J. Am. Chem. Soc.*, 1971, **93**, 3095.
- [35] G. Henkelman, A. Arnaldsson, H. Jónsson, *Comput. Mater. Sci.*, 2006, **36**, 354.
- [36] S. Gudmundsdóttir, W. Tang, G. Henkelman, H. Jónsson, E. Skúlason, *J. Chem. Phys.*, 2012, **137**, 164705.
- [37] <http://theory.cm.utexas.edu/bader/> (accessed July 2011).

- [38] A. Kokalj, *Comp. Mater. Sci.*, 2003, **28**, 155. Code available from <http://www.xcrysden.org/>
- [39] C. Kittel, "Introduction to Solid State Physics", Third ed., New York; Wiley, 1967.



decoration of step-edges of
HOPG by Ag, Au and Pt:
experiment and theory

118x77mm (72 x 72 DPI)